REVIEWS OF MODERN PHYSICS, VOLUME 82, APRIL–JUNE 2010

Feshbach resonances in ultracold gases

Cheng Chin

Department of Physics and James Franck Institute, University of Chicago, Chicago, Illinois 60637, USA

Rudolf Grimm

Center for Quantum Physics and Institute of Experimental Physics, University of Innsbruck, Technikerstraße 25, 6020 Innsbruck, Austria and Institute for Quantum Optics and Quantum Information, Austrian Academy of Sciences, Otto-Hittmair-Platz 1, 6020 Innsbruck, Austria

Paul Julienne and Eite Tiesinga

Joint Quantum Institute, National Institute of Standards and Technology and University of Maryland, 100 Bureau Drive, Gaithersburg, Maryland 20899-8423, USA

(Published 29 April 2010)

Feshbach resonances are the essential tool to control the interaction between atoms in ultracold quantum gases. They have found numerous experimental applications, opening up the way to important breakthroughs. This review broadly covers the phenomenon of Feshbach resonances in ultracold gases and their main applications. This includes the theoretical background and models for the description of Feshbach resonances, the experimental methods to find and characterize the resonances, a discussion of the main properties of resonances in various atomic species and mixed atomic species systems, and an overview of key experiments with atomic Bose-Einstein condensates, degenerate Fermi gases, and ultracold molecules.

DOI: 10.1103/RevModPhys.82.1225 PACS number(s): 03.75.−b, 34.50.Cx, 67.85.−d

CONTENTS

I. Introduction 1226
A. Ultracold gases and Feshbach resonances: Scope of the review 1226
B. Basic physics of a Feshbach resonance 1226
C. Historical remarks 1228
II. Theoretical Background 1229
A. Basic collision physics 1229
1. Collision channels 1230
2. Collision rates 1231
3. Resonance scattering 1231
B. Basic molecular physics 1233
1. van der Waals bound states and scattering 1234
2. Entrance- and closed channel dominated resonances: Resonance strength 1236
3. Coupled-channel picture of molecular interactions 1237
4. Classification and molecular physics of Feshbach resonances 1238
5. Some examples of resonance properties 1239
C. Simplified models of resonance scattering 1242
1. Contact potential model 1242
2. Other approximations 1243
3. van der Waals resonance model 1243
4. Analytic two-channel square well model 1243
5. Properties of Feshbach molecules 1244
III. Finding and Characterizing Feshbach Resonances 1245
A. Experimental methods 1245
1. General considerations 1245
a. What is the magnetic field range to be explored? 1245
b. What is the required magnetic field resolution? 1246
c. How to trap atoms for collision studies? 1246
d. How low a temperature is needed to observe the resonances? 1246
2. Inelastic loss spectroscopy 1246
3. Elastic collisions 1247
4. Radiative Feshbach spectroscopy 1247
5. Binding energy measurements 1248
B. Homonuclear alkali-metal systems 1248
1. Lithium 1249
2. Sodium 1250
3. Potassium 1250
4. Rubidium 1250
5. Cesium 1251
C. Heteronuclear and other systems 1251
1. Chromium 1252
2. Mixed species 1252
3. Isotopic mixtures 1253
IV. Control of Atomic Quantum Gases 1254
A. Bose-Einstein condensates 1254
1. Attainment of BEC 1254
2. Condensate mean field 1255
3. Controlled collapse and bright solitons 1255
4. Noninteracting condensates 1256
B. Degenerate Fermi gases 1257
1. BEC of molecules 1257
2. BEC-BCS crossover and fermion superfluidity 1258

V. Ultracold Feshbach Molecules 1260
A. Formation 1260
1. Feshbach ramps 1260
2. Oscillatory fields 1262
3. Atom-molecule thermalization 1262
B. Properties 1263
1. Dissociation and detection 1263
2. Halo dimers 1264
3. Collision properties 1264
4. Internal state transfer 1265
VI. Related Topics 1266
A. Optical Feshbach resonances 1266
1. Analogies 1266
2. Observations in alkali systems 1267
3. Prospects in alkaline-earth systems 1268
B. Feshbach resonances in optical lattices 1268
1. Atom pairs and molecules 1268
2. Reduced dimensional scattering 1270
3. Scattering in shallow lattices 1271
C. Efimov states and universal few-body physics 1271
1. Efimov's scenario 1271
2. Observations in ultracold cesium 1272
3. Prospects in few-body physics 1273
D. Molecular resonances and cold chemistry 1274
Acknowledgments 1275
Appendix: Tables of Selected Resonances 1275
References 1277

I. INTRODUCTION

A. Ultracold gases and Feshbach resonances: Scope of the review

The impact of ultracold atomic and molecular quantum gases on present-day physics is linked to the extraordinary degree of control that such systems offer to investigate the fundamental behavior of quantum matter under various conditions. The interest goes beyond atomic and molecular physics, reaching far into other fields, such as condensed matter and few- and many-body physics. In all these applications, Feshbach resonances represent the essential tool to control the interaction between the atoms, which has been the key to many breakthroughs.

Ultracold gases are generally produced by laser cooling (Metcalf and van der Straten, 1999) and subsequent evaporative cooling (Ketterle and van Druten, 1997). At temperatures in the nanokelvin range and typical number densities somewhere between 10^{12} and 10^{15} cm^{-3}, quantum-degenerate states of matter are formed when the atomic de Broglie wavelength exceeds the typical interparticle distance and quantum statistics governs the behavior of the system. The attainment of Bose-Einstein condensation (BEC) in dilute ultracold gases marked the starting point of a new era in physics (Anderson *et al.*, 1995; Bradley *et al.*, 1995; Davis *et al.*, 1995), and degenerate atomic Fermi gases entered the stage a few years later (DeMarco *et al.*, 1999; Schreck *et al.*, 2001; Truscott *et al.*, 2001). The developments of the techniques to cool and trap atoms by laser light were recognized with the 1997 Nobel prize in physics (Chu, 1998; Cohen-Tannoudji, 1998; Phillips, 1998). Only four years later, the achievement of BEC in dilute gases of alkali atoms and early fundamental studies of the properties of the condensates led to the 2001 Nobel prize (Cornell and Wieman, 2002; Ketterle, 2002).[1]

In this review, we give a broad coverage of Feshbach resonances in view of the manifold applications they have found in ultracold gases. Regarding theory, we focus on the underlying two-body physics and on models to describe Feshbach resonances. In the experimental part, we include applications to few- and many-body physics; we discuss typical or representative results instead of the impossible attempt to exhaustively review all developments in this rapidly growing field. Several aspects of Feshbach resonances and related topics have already been reviewed elsewhere. An early review on Feshbach resonance theory was given by Timmermans *et al.* (1999). In another theoretical review, Duine and Stoof (2004) focused on atom-molecule coherence. Hutson and Soldán (2006) and Köhler *et al.* (2006) reviewed the formation of ultracold molecules near Feshbach resonances. The closely related topic of photoassociation was reviewed by Jones *et al.* (2006).

In Sec. II, we start with a presentation of the theoretical background. Then, in Sec. III, we present the various experimental methods to identify and characterize Feshbach resonances. There we also discuss the specific interaction properties of different atomic species, which can exhibit vastly different behaviors. In Sec. IV, we present important applications of interaction control in experiments on atomic Bose and Fermi gases. In Sec. V, we discuss properties and applications of ultracold molecules created via Feshbach association. Finally, in Sec. VI, we discuss some related topics, such as optical Feshbach resonances, interaction control in optical lattices, few-body physics, and the relation to molecular scattering resonances and cold chemistry.

B. Basic physics of a Feshbach resonance

The physical origin and the elementary properties of a Feshbach resonance can be understood from a simple picture. Here we outline the basic ideas, whereas in Sec. II we provide a more detailed theoretical discussion.

We consider two molecular potential curves $V_{\mathrm{bg}}(R)$ and $V_c(R)$, as shown in Fig. 1. For large internuclear distances R, the background potential $V_{\mathrm{bg}}(R)$ asymptotically connects to two free atoms in the ultracold gas. For a collision process, having small energy E, this potential represents the energetically open channel, in the follow-

[1]For overviews on laser cooling and trapping, BEC, and ultracold Fermi gases see the proceedings of the Varenna summer schools in 1991, 1998, and 2006 (Arimondo *et al.*, 1992; Inguscio *et al.*, 1999, 2008). For reviews on the theory of degenerate quantum gases of bosons and fermions see Dalfovo *et al.* (1999) and Giorgini *et al.* (2008), respectively, and Stringari and Pitaevskii (2003) and Pethick and Smith (2008).

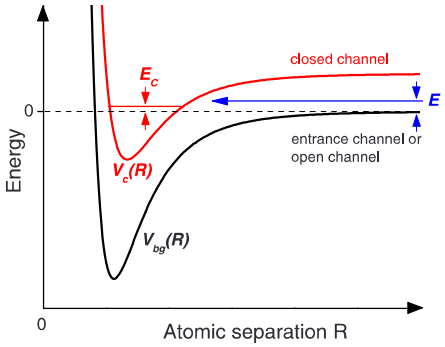

FIG. 1. (Color online) Basic two-channel model for a Feshbach resonance. The phenomenon occurs when two atoms colliding at energy E in the entrance channel resonantly couple to a molecular bound state with energy E_c supported by the closed channel potential. In the ultracold domain, collisions take place near zero energy, $E \to 0$. Resonant coupling is then conveniently realized by magnetically tuning E_c near 0 if the magnetic moments of the closed and open channels differ.

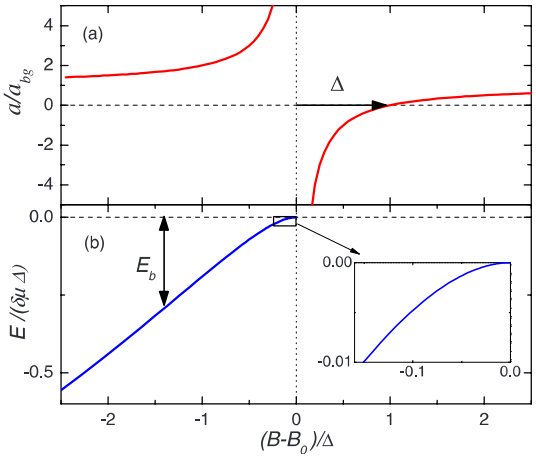

FIG. 2. (Color online) Feshbach resonance properties. (a) Scattering length a and (b) molecular state energy E near a magnetically tuned Feshbach resonance. The binding energy is defined to be positive, $E_b = -E$. The inset shows the universal regime near the point of resonance where a is very large and positive.

ing referred to as the entrance channel. The other potential $V_c(R)$, representing the closed channel, is important as it can support bound molecular states near the threshold of the open channel.

A Feshbach resonance occurs when the bound molecular state in the closed channel energetically approaches the scattering state in the open channel. Then even weak coupling can lead to strong mixing between the two channels. The energy difference can be controlled via a magnetic field when the corresponding magnetic moments are different. This leads to a magnetically tuned Feshbach resonance. The magnetic tuning method is the common way to achieve resonant coupling and it has found numerous applications, as discussed in this review. Alternatively, resonant coupling can be achieved by optical methods, leading to optical Feshbach resonances with many conceptual similarities to the magnetically tuned case (see Sec. VI.A). Such resonances are promising for cases where magnetically tunable resonances are absent.

A magnetically tuned Feshbach resonance can be described by a simple expression,[2] introduced by Moerdijk *et al.* (1995), for the s-wave scattering length a as a function of the magnetic field B,

$$a(B) = a_{\rm bg}\left(1 - \frac{\Delta}{B - B_0}\right). \tag{1}$$

Figure 2(a) shows this resonance expression. The background scattering length $a_{\rm bg}$, which is the scattering length associated with $V_{\rm bg}(R)$, represents the off-resonant value. It is directly related to the energy of the last-bound vibrational level of $V_{\rm bg}(R)$. The parameter B_0 denotes the resonance position, where the scattering length diverges ($a \to \pm\infty$), and the parameter Δ is the resonance width. Note that both $a_{\rm bg}$ and Δ can be positive or negative. An important point is the zero crossing of the scattering length associated with a Feshbach resonance; it occurs at a magnetic field $B = B_0 + \Delta$. Note also that we use G as the magnetic field unit in this paper because of its near-universal usage among groups working in this field, 1 G $= 10^{-4}$ T.

The energy of the weakly bound molecular state near the resonance position B_0 is shown in Fig. 2(b) relative to the threshold of two free atoms with zero kinetic energy. The energy approaches threshold at $E = 0$ on the side of the resonance where a is large and positive. Away from resonance, the energy varies linearly with B with a slope given by $\delta\mu$, the difference in magnetic moments of the open and closed channels. Near resonance the coupling between the two channels mixes in entrance-channel contributions and strongly bends the molecular state.

In the vicinity of the resonance position at B_0, where the two channels are strongly coupled, the scattering length is very large. For large positive values of a, a "dressed" molecular state exists with a binding energy given by

$$E_b = \hbar^2/2\mu a^2, \tag{2}$$

where μ is the reduced mass of the atom pair. In this limit E_b depends quadratically on the magnetic detuning $B - B_0$ and results in the bend shown in the inset of Fig. 2. This region is of particular interest because of its universal properties; here the state can be described in terms of a single effective molecular potential having scattering length a. In this case, the wave function for the relative atomic motion is a quantum halo state which extends to a large size on the order of a; the molecule is then called a halo dimer (see Sec. V.B.2).

[2]This simple expression applies to resonances without inelastic two-body channels. Some Feshbach resonances, especially the optical ones, feature two-body decay. For a more general discussion including inelastic decay see Sec. II.A.3.

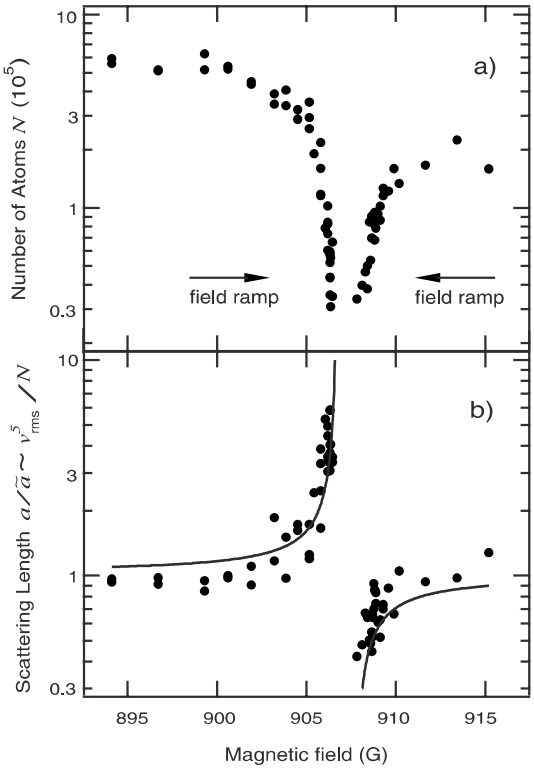

FIG. 3. Observation of a magnetically tuned Feshbach resonance in an optically trapped BEC of Na atoms. The upper panel shows a strong loss of atoms near the resonance, which is due to enhanced three-body recombination. The lower panel shows the dispersive shape of the scattering length a near the resonance, as determined from measurements of the mean-field interaction by expansion of the condensate after release from the trap; here a is normalized to the background value a_{bg}. From Inouye *et al.*, 1998.

A useful distinction can be made between resonances that exist in various systems (see Sec. II.B.2). For narrow resonances with a width Δ typically well below 1 G (see the Appendix) the universal range persists only for a very small fraction of the width. In contrast, broad resonances with a width typically much larger than 1 G tend to have a large universal range extending over a considerable fraction of the width. The first class of resonances is referred to as closed-channel dominated resonances, whereas the second class is called entrance-channel dominated resonances. For the distinction between both classes, the width Δ is not the only relevant parameter. Also the background scattering length a_{bg} and the differential magnetic moment $\delta\mu$ need to be taken into account. Section II.B.2 discusses this important distinction in terms of a dimensionless resonance strength.

Figure 3 shows the observation of a Feshbach resonance as reported by Inouye *et al.* (1998) for an optically trapped BEC of Na atoms. This early example highlights the two most striking features of a Feshbach resonance, the tunability of the scattering length according to Eq. (1) and the fast loss of atoms in the resonance region. The latter can be attributed to strongly enhanced three-body recombination and molecule formation near a Feshbach resonance (see Sec. III.A.2).

A Feshbach resonance in an ultracold atomic gas can serve as a gateway into the molecular world and is thus strongly connected to the field of ultracold molecules (see Sec. V). Various techniques have been developed to associate molecules near Feshbach resonances. Ultracold molecules produced in this way are commonly referred to as *Feshbach molecules*. The meaning of this term is not precisely defined, as Feshbach molecules can be transferred to many other states near threshold or to much more deeply bound states, thus being converted to more conventional molecules. We use the term Feshbach molecule for any molecule that exists near the threshold in an energy range set by the quantum of energy for near-threshold vibrations. The universal halo state is a special very weakly bound case of a Feshbach molecule.

C. Historical remarks

Early investigations on phenomena arising from the coupling of a bound state to the continuum go back to the 1930s. Rice (1933) considered how a bound state predissociates into a continuum, Fano (1935) and Fano *et al.* (2005) described asymmetric line shapes occurring in such a situation as a result of quantum interference, and Beutler (1935) reported on the observation of highly asymmetric line shapes in rare gas photoionization spectra. Nuclear physicists considered basically the same situation, having nuclear scattering experiments in mind instead of atomic physics. Breit and Wigner (1936) considered the situation in the limit when the bound state plays a dominant role and the asymmetry disappears. Later interference and line-shape asymmetry were taken into account by several authors (Blatt and Weisskopf, 1952).

Feshbach (1917–2000) and Fano (1912–2001) developed their thorough treatments of the resonance phenomena that arise from the coupling of a discrete state to the continuum. Their work was carried out independently using different theoretical approaches. While Feshbach's work originated in the context of nuclear physics (Feshbach, 1958, 1962), Fano approached the problem on the background of atomic physics (Fano, 1961). reformulating and extending his earlier work (Fano, 1935; Fano *et al.*, 2005). Nowadays, the term "Feshbach resonance" is most widely used in the literature for the resonance phenomenon itself, but sometimes also the term "Fano-Feshbach resonance" appears. As a curiosity Feshbach himself considered his name being attached to a well-known resonance phenomenon as a mere atomic physics jargon (Kleppner, 2004; Rau, 2005). Fano's name is usually associated with the asymmetric line shape of such a resonance, well known in atomic physics as a "Fano profile."

A prominent example for the observation of a Feshbach resonance in atomic physics is the experiment of Bryant *et al.* (1977) on photodetachment by the negative ion of hydrogen. Near a photon energy of 11 eV two

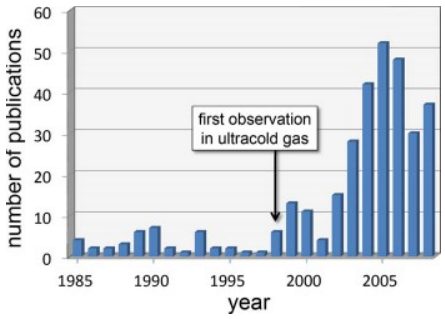

FIG. 4. (Color online) Number of publications per year (from 1985 to 2008) with Feshbach resonances appearing in the title. Data from ISI Web of Science.

prominent resonances were seen, one of them being a Feshbach resonance and the other one a "shape resonance" (see Sec. II.A.3). Many more situations where Feshbach resonances play an important role can be found in atomic, molecular, and chemical physics [see Spence and Noguchi (1975), Gauyacq and Herzenberg (1982), MacArthur *et al.* (1985), Nieh and Valentini (1990), and Weber *et al.* (1999) for a few examples]. In such experiments, the resonances occur when the scattering energy is varied. This is in contrast to the experiments on ultracold gases, where scattering takes place in the zero-energy limit and the resonances occur when an external field tunes bound states near threshold.

In the context of quantum gases, Feshbach resonances were first considered by Stwalley (1976), who suggested the existence of magnetically induced Feshbach resonances in the scattering of spin-polarized hydrogen and deuterium atoms (H+D and D+D). He pointed to enhanced inelastic decay near these resonances and suggested that they should be avoided to maintain stable spin-polarized hydrogen gases. A related loss resonance in hydrogen was observed by Reynolds *et al.* (1986). The positive aspect of such resonances was first pointed out by Tiesinga *et al.* (1993), who showed that they can be used to change the sign and strength of the interaction between ultracold atoms. In 1998, the possibility of interaction tuning via Feshbach resonances was demonstrated by Inouye *et al.* (1998) for a ^{23}Na BEC, as already discussed in the preceding section. In the same year, Courteille *et al.* (1998) demonstrated a Feshbach resonance in a trapped sample of ^{85}Rb atoms through the enhancement of photoassociative loss induced by a probe laser.

The important role of Feshbach resonances in present-day quantum gas experiments can be highlighted by looking at the number of publications per year with Feshbach resonances in the title (see Fig. 4). Before 1998, one finds just a few publications with the majority not related to ultracold atoms. Then, after 1998, a substantial increase is observed as a result of the first successful experiments with Feshbach resonances in ultracold gases. It then took a few years until Feshbach resonances had become a fully established tool and opened up many new applications in the field. This is reflected in the steep increase of the publication rate in the period from 2002 to 2004.

II. THEORETICAL BACKGROUND

This review primarily concentrates on magnetically tunable resonances, described in the next sections, while Sec. VI.A discusses optical changes in scattering lengths. Here we describe the two-body physics of collision resonances, not the few- or many-body aspects. Properties of a number of magnetic Feshbach resonances are tabulated in the Appendix.

A. Basic collision physics

The theory for describing two-body collisions is described in a number of textbooks (Mott and Massey, 1965; Messiah, 1966; Taylor, 1972). First consider the collision of two structureless atoms, labeled 1 and 2 with masses m_1 and m_2 interacting under the influence of the potential $V(\mathbf{R})$, where $\mathbf{R}$ is the vector between the positions of the two atoms with magnitude R. The separated atoms are prepared in a plane wave with relative kinetic energy $E=\hbar^2k^2/(2\mu)$ and relative momentum $\hbar\mathbf{k}$, where $\mu=m_1m_2/(m_1+m_2)$ is the reduced mass of the pair. The plane wave in turn is expanded in a standard sum over spherical harmonic functions $Y_{\ell m_\ell}(\hat{\mathbf{R}})$, where ℓ is the relative angular momentum, m_ℓ is its projection along a space fixed z axis, and $\hat{\mathbf{R}}=\mathbf{R}/R$ is the direction vector on the unit sphere (Messiah, 1966). This expansion is called the partial wave expansion, and the various partial waves $\ell=0,1,2,\ldots$ are designated $s,p,d,\ldots$ waves.

If the potential $V(\mathbf{R})$ is isotropic, depending only on the magnitude of $\mathbf{R}$, there is no coupling among partial waves, each of which is described by the solution $\psi_\ell(R)=\phi_\ell(R)/R$ to the Schrödinger equation

$$-\frac{\hbar^2}{2\mu}\frac{d^2\phi_\ell(R)}{dR^2}+V_\ell(R)\phi_\ell(R)=E\phi_\ell(R), \tag{3}$$

where $V_\ell(R)=V(R)+\hbar^2\ell(\ell+1)/(2\mu R^2)$ includes the centrifugal potential, which is repulsive for $\ell>0$ and vanishes for the s wave. We assume $V(R)\to 0$ as $R\to\infty$, so that E represents the energy of the separated particles. This equation has a spectrum of N_ℓ bound state solutions at discrete energies $E_{n\ell}$ for $E<0$ and a continuous spectrum of scattering states with $E>0$. While bound states are normally labeled by vibrational quantum number $v=0,\ldots,N_\ell-1$ counting up from the bottom of the potential, we prefer to label threshold bound states by quantum number $n=-1,-2,\ldots$ counting down from the top of the potential for the last, next to last, etc. bound states. The bound state solutions $|n\ell\rangle$ are normalized to unity, $|\langle n\ell|n\ell\rangle|^2=1$, and $\phi_{n\ell}(R)=\langle R|n\ell\rangle\to 0$ as $R\to\infty$. The scattering solutions, representing the incident plane wave plus a scattered wave, approach

$$\phi_\ell(R,E) \to c\frac{\sin[kR-\pi\ell/2+\eta_\ell(E)]}{\sqrt{k}}e^{i\eta_\ell(E)} \quad (4)$$

as $R\to\infty$, where $\eta_\ell(E)$ is the scattering phase shift and $c=\sqrt{2\mu/\pi\hbar^2}$ is a constant that ensures the wave function $|E\ell\rangle$ is normalized per unit energy, $\langle E\ell|E'\ell\rangle = \int_0^\infty \phi_\ell^*(R,E)\phi_\ell(R,E')dR=\delta(E-E')$. The scattering phase shift is the key parameter that incorporates the effect of the whole potential on the collision event.

Sadeghpour *et al.* (2000) reviewed the special properties of scattering phase shift near a collision threshold when $k\to 0$. If $V(R)$ varies as $1/R^s$ at large R, then $\tan\eta_\ell \propto k^{2\ell+1}$ if $2\ell+1\leqslant s-2$ and $\tan\eta_\ell\propto k^{s-2}$ if $2\ell+1\geqslant s-2$. While Levinson's theorem shows that $\eta_\ell\to N_\ell\pi$ as $k\to 0$, we need not consider the $N_\ell\pi$ part of the phase shift in this review. For van der Waals potentials with $s=6$, the threshold $\tan\eta_\ell$ varies as k and k^3 for s and p waves and as k^4 for all other partial waves. The properties of s-wave collisions are of primary interest for cold neutral atom collisions, where near threshold, a more precise statement of the variation of $\tan\eta_0$ with k is given by the effective range expansion,

$$k\cot\eta_0(E) = -1/a + \tfrac{1}{2}r_0k^2, \quad (5)$$

where a is called the s-wave scattering length and r_0 is the effective range. For practical purposes, it often suffices to retain only the scattering length term and use $\tan\eta_0(E)=-ka$. Depending on the potential, the scattering length can have any value, $-\infty<a<+\infty$.

When the scattering length is positive and sufficiently large, that is, large compared to the characteristic length scale of the molecular potential (see Sec. II.B.1), the last s-wave bound state of the potential, labeled by index $n=-1$ and $\ell=0$, is just below threshold with a binding energy $E_b=-E_{-1,0}$ given by Eq. (2) in the Introduction. The domain of universality, where scattering and bound state properties are solely characterized by the scattering length and mass, is discussed in recent reviews (Braaten and Hammer, 2006; Köhler *et al.*, 2006). The universal bound state wave function takes on the form $\phi_{-1,0}(R)=\sqrt{2/a}\exp(-R/a)$ at large R. Such a state exists almost entirely at long range beyond the outer classical turning point of the potential. Such a bound state is known as a "halo state," also studied in nuclear physics (Riisager, 1994) and discussed in Sec. V.B.2.

1. Collision channels

The atoms used in cold collision experiments generally have spin structure. For each atom $i=1$ or 2 in a collision the electronic orbital angular momentum $\mathbf{L}_i$ is coupled to the total electronic spin angular momentum $\mathbf{S}_i$ to give a resultant $\mathbf{j}_i$, which in turn is coupled to the nuclear spin $\mathbf{I}_i$ to give the total angular momentum $\mathbf{f}_i$. The eigenstates of each atom are designated by the composite labels q_i. At zero magnetic field these labels are f_im_i, where m_i is the projection of $\mathbf{f}_i$. For example, alkali-metal atoms that are commonly used in Feshbach resonance experiments have $^2S_{1/2}$ electronic ground states with quantum numbers $L_i=0$ and $S_i=1/2$, for which there are only two values of $f_i=I_i-1/2$ and $I_i+1/2$ when $I_i\neq 0$. Whether f_i is an integer or half an odd integer determines whether the atom is a composite boson or fermion.

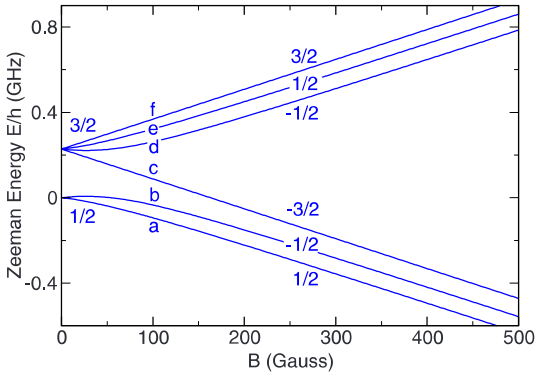

FIG. 5. (Color online) Atomic energy levels of the ^{6}Li atom, which has $S=1/2$, $I=1$, and $f=1/2$ and 3/2. The figure shows both the projection m of f and the alphabetical shorthand notation q_i=a, b, c, d, e, and f used to label the levels in order of increasing energy.

A magnetic field $\mathbf{B}$ splits these levels into a manifold of Zeeman sublevels. Only the projection m_i along the field remains a good quantum number, and $B=0$ levels with the same m_i but different f_i can be mixed by the field. Even at high field, where the individual f_i values no longer represent good quantum numbers, the f_i value still can be retained as a label, indicating the value at $B=0$ with which the level adiabatically correlates.

Figure 5 shows the Zeeman energy levels versus B for the ^{6}Li atom, a fermion, according to the classic Breit-Rabi formula (Breit and Rabi, 1931). The two f_i levels are split at $B=0$ by the hyperfine energy, $E_{\rm hf}/h=228$ MHz. At large fields the lower group of three levels is associated with the quantum number $m_S=-1/2$, while the upper group has $m_S=+1/2$. The figure also shows our standard notation for atomic Zeeman levels for any species and any field strength. We label states by lower case Roman letters a, b, c,… in order of increasing energy. Some prefer to label the levels in order numerically as 1, 2, 3… . The notation q_i can symbolically refer to the f_im_i, alphabetical, or numerical choice of labeling

The collision event between two atoms is defined by preparing the atoms in states q_1 and q_2 while they are separated by a large distance R, then allowing them to come together, interact, and afterward separate to two atoms in states q_1' and q_2'. If the two final states are the same as the initial ones, $q_1,q_2=q_1',q_2'$, the collision is said to be elastic, and the atoms have the same relative kinetic energy E before and after the collision. If one of the final states is different from an initial state, the collision is said to be inelastic. This often results in an energy release that causes a loss of cold atoms when the energetic atoms escape from the shallow trapping potential. We concentrate primarily on collisions where the

two-body inelastic collision rate is zero or else very small in comparison to the elastic rate since this corresponds in practice to most cases of practical experimental interest. This condition is necessary for efficient evaporative cooling or to prevent rapid decay of the cold gas. Section III.A.2 discusses how atom loss due to three-body collisions can be used to detect the presence of two-body resonances.

In setting up the theory for the collision of two atoms, the scattering channels are defined by the internal states of the two atoms 1 and 2 and the partial wave, $|\alpha\rangle = |q_1 q_2\rangle |\ell m_\ell\rangle$, where $\langle \hat{R} | \ell m_\ell \rangle = Y_{\ell m_\ell}(\hat{\mathbf{R}})$. Since for collisions in a magnetic field the quantum number $M = m_1 + m_2 + m_\ell$ is strictly conserved, a scattering channel can be conveniently labeled by specifying the set of quantum numbers $\{q_1 q_2 \ell M\}$. For s waves, where $\ell = m_\ell = 0$ and $M = m_1 + m_2$, it is only necessary to specify the quantum numbers $\{q_1 q_2\}$ to label a channel.

When the two atoms are of the same isotopic species, the wave function must be symmetric (antisymmetric) with respect to exchange of identical bosons (fermions). We assume such symmetrized and normalized functions as described by Stoof *et al.* (1988). Exchange symmetry ensures that identical atoms in identical spin states can only collide in $s, d, \ldots$ waves for the case of bosons and in $p, f, \ldots$ waves in the case of fermions; in all other cases, collisions in all partial waves are allowed.

The channel energy $E_\alpha = E(q_1) + E(q_2)$ is the internal energy of the separated atoms. Assume that the atoms are prepared in channel α with relative kinetic energy E so that the total energy is $E_{\rm tot} = E_\alpha + E$. Any channel β with $E_\beta \leqslant E_{\rm tot}$ is called an open channel and any channel with $E_\beta > E_{\rm tot}$ is called a closed channel. A collision can produce atoms in an open channel after the collision, but not in a closed channel, since the atoms do not have enough energy to separate to the product atoms.

2. Collision rates

The partial collision cross section for starting in open channel α with relative kinetic energy E and ending in open channel β can be expressed in terms of the $S_{\alpha,\beta}(E)$ element of the multichannel unitary scattering matrix $\mathbf{S}$. The cross section for elastic scattering at energy E in channel α is

$$\sigma_{{\rm el},\alpha}(E) = g_\alpha (\pi/k^2) |1 - S_{\alpha,\alpha}(E)|^2, \tag{6}$$

whereas the unitarity property of $\mathbf{S}$ allows us to express the cross section for loss of atoms from channel α as

$$\sigma_{{\rm loss},\alpha}(E) = g_\alpha (\pi/k^2) [1 - |S_{\alpha,\alpha}(E)|^2]. \tag{7}$$

The corresponding partial elastic and inelastic rate coefficients $K_{{\rm el},\alpha}(E)$ and $K_{{\rm loss},\alpha}(E)$ are found by multiplying these partial cross sections by the relative collision velocity $v = \hbar k/\mu$. The factor $g_\alpha = 1$ except for certain special cases involving identical particles. The factor $g_\alpha = 2$ for describing thermalization or inelastic collisions in a normal Maxwellian gas of two atoms of the same species in identical spin states. Inelastic decay of a pure Bose-Einstein condensate has $g_\alpha = 1$ (Kagan *et al.*, 1985; Stoof *et al.*, 1989).

If only one open channel α is present, collisions are purely elastic and $S_{\alpha,\alpha}(E) = \exp[2i\eta_\alpha(E)]$. For s waves the real-valued $\tan \eta_\alpha(E) \to -k a_\alpha$ as $k \to 0$ and a_α is the scattering length for channel α. When other open channels are present, the amplitude $|S_{\alpha,\alpha}(E)|$ is no longer unity, and for s wave we can represent the complex phase $\eta_\alpha(E) \to -k\tilde{a}_\alpha$ for $k \to 0$ in terms of a complex scattering length (Bohn and Julienne, 1996; Balakrishnan *et al.*, 1997)

$$\tilde{a}_\alpha = a_\alpha - i b_\alpha, \tag{8}$$

where a and b are real, and $1 - |S_{\alpha,\alpha}(E)|^2 \to 4k b_\alpha \geqslant 0$ as $k \to 0$. The threshold behavior is

$$\sigma_{{\rm el},\alpha}(E) = 4\pi g_\alpha (a_\alpha^2 + b_\alpha^2) \tag{9}$$

for the s-wave elastic collision cross section and

$$K_{{\rm loss},\alpha}(E) = (2h/\mu) g_\alpha b_\alpha \tag{10}$$

for inelastic collisions that remove atoms from channel α. Both $\sigma_{{\rm el},\alpha}$ and $K_{{\rm loss},\alpha}$ approach constant values when E is sufficiently small.

The unitarity property of the S matrix also sets an upper bound on the cross sections. Since there is a rigorous upper bound of $|S_{\alpha,\alpha}(E)| \leqslant 1$, we find that the elastic scattering cross section is maximum,

$$\sigma_{{\rm el},\alpha}(E) = (4\pi/k^2) g_\alpha, \tag{11}$$

for any channel α (and thus any partial wave ℓ) when $S_{\alpha,\alpha}(E) = -1$. Furthermore, $\sigma_{{\rm loss},\alpha}(E)$, if nonvanishing, has a maximum value of $\sigma_{{\rm loss},\alpha}(E) = g_\alpha \pi/k^2$ when $S_{\alpha,\alpha}(E) = 0$. These limits are called the unitarity limits of the cross sections. For s-wave collisions this limit is approached at quite low energy given by $E \approx \hbar^2/(2\mu a_\alpha^2)$, where $k a_\alpha \approx 1$.

In order to compare with experimental data the partial rate coefficients must be summed over partial waves and thermally averaged over the distribution of relative collision velocities at temperature T. This defines the total rate coefficients $K_{{\rm el},q_1 q_2}(T)$ and $K_{{\rm loss},q_1 q_2}(T)$ when the atoms are prepared in states q_1 and q_2, respectively. Often the temperatures are sufficiently small that only the s-wave entrance channel contributes.

3. Resonance scattering

The idea of resonance scattering in atomic and molecular systems has been around since the earliest days of quantum physics, as described in the Introduction. A conventional "resonance" occurs when the phase shift changes rapidly by $\approx \pi$ over a relatively narrow range of energy due to the presence of a quasibound level of the system that is coupled to the scattering state of the colliding atoms. Such a resonance may be due to a quasibound level trapped behind a repulsive barrier of a single potential or may be due to some approximate bound state which has a different symmetry and potential from that of the colliding atoms. The former is commonly known as a shape resonance, whereas the latter is

often called a Feshbach resonance, in honor of Herman Feshbach, who developed a theory and a classification scheme for resonance scattering phenomena in the context of nuclear physics (Feshbach, 1958, 1962). We will follow here Fano's configuration interaction treatment of resonant scattering (Fano, 1961), which is common in atomic physics. A variety of treatments of the two-body physics of resonances in the context of ultracold Bose gases has been given by Timmermans *et al.* (1999), Duine and Stoof (2004), Góral *et al.* (2004), Marcelis *et al.* (2004), and Raoult and Mies (2004).

We first consider the standard scattering picture away from any collision threshold defined by a two-channel Hamiltonian H. Assume that we can describe our system to a good approximation by two uncoupled "bare" channels, as schematically shown in Fig. 1. One is the open background scattering channel $|\mathrm{bg}\rangle$ with scattering states $|E\rangle = \phi_{\mathrm{bg}}(R,E)|\mathrm{bg}\rangle$ labeled by their collision energy E. The other is the closed channel $|c\rangle$ supporting a bound state $|C\rangle = \phi_c(R)|c\rangle$ with eigenenergy E_c. The functions $\phi_c(R)$ and $\phi_{\mathrm{bg}}(R,E)$ are the solutions to Eq. (3) for the background potential $V_{\mathrm{bg}}(R)$ and the closed channel potential $V_c(R)$, respectively. Here $\phi_c(R)$ is normalized to unity. The scattering in the open channel is characterized by a background phase shift $\eta_{\mathrm{bg}}(E)$. When the Hamiltonian coupling $W(R)$ between the two channels is taken into account, then the two states become mixed or dressed by the interaction, and the scattering phase picks up a resonant part due to the bound state embedded in the scattering continuum,

$$\eta(E) = \eta_{\mathrm{bg}}(E) + \eta_{\mathrm{res}}(E), \tag{12}$$

where $\eta_{\mathrm{res}}(E)$ takes on the standard Breit-Wigner form (Mott and Massey, 1965; Taylor, 1972),

$$\eta_{\mathrm{res}}(E) = -\tan^{-1}\left(\frac{\frac{1}{2}\Gamma(E_c)}{E - E_c - \delta E(E_c)}\right). \tag{13}$$

The interaction $W(R)$, which vanishes at large R, determines two key features of the resonance, namely, its width,

$$\Gamma(E) = 2\pi|\langle C|W(R)|E\rangle|^2, \tag{14}$$

and its shift δE to a new position at $E_c + \delta E(E)$,

$$\delta E(E) = \mathcal{P}\int_{-\infty}^{\infty} \frac{|\langle C|W(R)|E'\rangle|^2}{E - E'} dE', \tag{15}$$

where $\mathcal{P}$ implies a principal part integral, which includes a sum over the contribution from any discrete bound states in the spectrum of the background channel. When the resonance energy is not near the channel threshold, it is normally an excellent approximation to take the width and shift as energy-independent constants, $\Gamma(E_c)$ and $\delta E(E_c)$, evaluated at the resonance energy E_c, as in Eq. (13). The resonance phase changes by $\approx\pi$ when E varies over a range on the order of Γ from below to above resonance.

The essential difference between conventional and threshold resonance scattering is that if E_c is close to the open channel threshold at $E=0$, the explicit energy dependence of the width and shift become crucial (Bohn and Julienne, 1999; Marcelis *et al.*, 2004; Julienne and Gao, 2006),

$$\eta_{\mathrm{res}}(E) = -\tan^{-1}\left(\frac{\frac{1}{2}\Gamma(E)}{E - E_c - \delta E(E)}\right). \tag{16}$$

The threshold laws for the s-wave width and shift as $k \to 0$ are

$$\tfrac{1}{2}\Gamma(E) \to (ka_{\mathrm{bg}})\Gamma_0, \tag{17}$$

$$E_c + \delta E(E) \to E_0, \tag{18}$$

where Γ_0 and E_0 are E-independent constants. Since $\Gamma(E)$ is positive definite, Γ_0 has the same sign as a_{bg}. Combining these limits with the background phase property, $\eta_{\mathrm{bg}}(E) \to -ka_{\mathrm{bg}}$, and, for the sake of generality, adding a decay rate $\gamma/\hbar$ for the decay of the bound state into all available loss channels give in the limit of $k \to 0$

$$\tilde{a} = a - ib = a_{\mathrm{bg}} + \frac{a_{\mathrm{bg}}\Gamma_0}{-E_0 + i(\gamma/2)}. \tag{19}$$

The unique role of scattering resonances in the ultracold domain comes from the ability to tune the threshold resonance position E_0 through zero by varying either an external magnetic field with strength B or optical field with frequency ν.

Both magnetically and optically tunable resonances are treated by the same theoretical formalism given above, although the physical mechanisms determining the coupling and tuning are quite different. In the case of a magnetically tunable resonance, the channel can often be chosen so that γ is zero or small enough to be ignored, whereas optical resonances are always accompanied by decay processes γ due to decay of the excited state. The resonance strength Γ_0 is fixed for magnetic resonances, but $\Gamma_0(I)$ for optical resonances can be turned off and on by varying the laser intensity I. It may also be possible to gain some control over Γ_0 using a combination of electric and magnetic fields (Marcelis *et al.*, 2008).

In the case of a magnetically tunable resonance, there is a difference $\delta\mu = \mu_{\mathrm{atoms}} - \mu_c$ between the magnetic moment μ_{atoms} of the separated atoms and the magnetic moment μ_c of the bare bound state $|C\rangle$. Thus, the energy E_c of the state $|C\rangle$ relative to the channel energy of the separated atoms,

$$E_c = \delta\mu(B - B_c), \tag{20}$$

can be tuned by varying the magnetic field, and E_c is zero at a magnetic field equal to B_c. Then, given that $\gamma = 0$, the scattering length takes on the simple form given in Eq. (1),

$$a(B) = a_{\rm bg} - a_{\rm bg}\Delta/(B - B_0), \tag{21}$$

where

$$\Delta = \Gamma_0/\delta\mu \quad \text{and} \quad B_0 = B_c + \delta B \tag{22}$$

are the width and the position of the singularity in the scattering length, shifted due to the interaction between the closed and open channels by an amount $\delta B = -\delta E/\delta\mu$. Note that Δ has the same sign as $\delta\mu/a_{\rm bg}$. Figure 2 schematically shows the scattering length near the point of resonance B_0.

The complex scattering length of an optically tunable resonance at laser frequency ν includes the collisional loss due to excited state decay (Fedichev, Kagan, *et al.*, 1996; Bohn and Julienne, 1999),

$$\tilde{a}(\nu, I) = a_{\rm bg} + \frac{a_{\rm bg}\Gamma_0(I)}{h[\nu - \nu_c - \delta\nu(I)] + i(\gamma/2)}, \tag{23}$$

where the optically induced width $\Gamma_0(I)$ and shift $\delta\nu(I)$ are linear in I, and ν_c represents the frequency of the unshifted optical transition between the excited bound state and the collisional state of the two atoms at $E=0$.

Whenever bound state decay is present, whether for magnetically or optically tunable resonances, Eq. (19) shows that resonant control of the scattering length,

$$a = a_{\rm bg} - a_{\rm res}\frac{\gamma E_0}{E_0^2 + (\gamma/2)^2}, \tag{24}$$

is accompanied by collisional loss given by

$$b = \frac{1}{2}a_{\rm res}\frac{\gamma^2}{E_0^2 + (\gamma/2)^2}. \tag{25}$$

The resonant length parameter

$$a_{\rm res} = a_{\rm bg}\Gamma_0/\gamma \tag{26}$$

is useful for defining the strength of an optical resonance (Bohn and Julienne, 1997; Ciuryło *et al.*, 2005) or any other resonance with strong decay (Hutson, 2007). Figure 6 gives an example of such a resonance. The scattering length has its maximum variation of $a_{\rm bg} \pm a_{\rm res}$ at $E_0 = \pm\gamma/2$, where $b = a_{\rm res}$. Resonances with $a_{\rm res} \leqslant |a_{\rm bg}|$ only allow relatively small changes in scattering length, yet b remains large enough that they are typically accompanied by large inelastic rate coefficients. On the other hand, if $a_{\rm res} \gg |a_{\rm bg}|$, losses can be overcome by using large detuning since the change in scattering length is $a - a_{\rm bg} = -a_{\rm res}(\gamma/E_0)$ when $|E_0| \gg \gamma$, whereas $b/|a - a_{\rm bg}| = \frac{1}{2}|\gamma/E_0| \ll 1$.

The resonance length formalism is quite powerful. By introducing the idea of an energy-dependent scattering length (Blume and Greene, 2002; Bolda *et al.*, 2002) it can be extended to Feshbach resonances in reduced dimensional systems such as pancake or cigar-shaped optical lattice cells (Naidon and Julienne, 2006).

While this discussion has concentrated on resonant scattering properties for $E > 0$, the near-threshold resonant properties of bound Feshbach molecules for energy $E < 0$ are important aspects of Feshbach physics [see Fig. 2 and Köhler *et al.* (2006)]. In particular, as the bound state becomes more deeply bound, the closed channel character of the bound state increases and the binding energy E_b is no longer described by the universal expression in Eq. (2). The dressed or true molecular bound state of the system with energy $-E_b$ is a mixture of closed and background channel components,

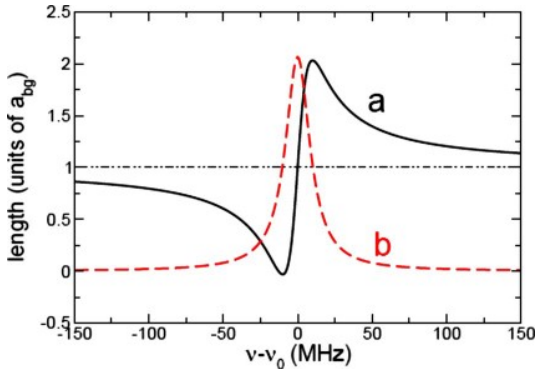

FIG. 6. (Color online) Scattering length for an optically tunable Feshbach resonance as a function of laser tuning $\nu - \nu_0$. The lengths a and b are defined in Eqs. (24) and (25). Here $a_{\rm bg} = 5.29$ nm, $\Gamma_0/h = 21$ MHz at $I = 500$ W/cm^2, $a_{\rm res} = 5.47$ nm, and $\gamma/h = 20$ MHz. Numerical values for the strength and spontaneous linewidth of the resonance are typical for ^{87}Rb and are taken from Fig. 1 of Theis *et al.*, 2004.

$$|\psi_b(R)\rangle = \sqrt{Z}\phi_c(R)|c\rangle + \chi_{\rm bg}(R)|{\rm bg}\rangle, \tag{27}$$

where $0 \leqslant Z \leqslant 1$ represents the fraction of the eigenstate $|\psi_b(R)\rangle$ in the closed channel component (Duine and Stoof, 2003). Unit normalization of $|\psi_b(R)\rangle$ ensures that $\int|\chi_{\rm bg}(R)|^2 dR = 1 - Z$. Since the variation of the energy $-E_b$ with a parameter x of the Hamiltonian satisfies the Hellman-Feynmann theorem $\partial(-E_b)/\partial x = \langle\psi_b|\partial H/\partial x|\psi_b\rangle$, it follows from Eq. (27) that

$$Z = \partial(-E_b)/\partial E_c = \delta\mu_b/\delta\mu. \tag{28}$$

Here $\delta\mu_b = \partial E_b/\partial B = \mu_{\rm atoms} - \mu_b$ is the difference between the magnetic moment of the separated atoms and the magnetic moment μ_b of the dressed molecular eigenstate. Since $\delta\mu_b$ vanishes in the limit $B \to B_0$, where $E_b \to 0$ according to the universality condition in Eq. (2), then Z vanishes in this limit also. Section II.C.5 develops more specific properties and conditions for E_b and Z in this limit.

B. Basic molecular physics

Most atoms that can be trapped at ultracold temperatures have ground S states with zero electronic orbital angular momentum ($L=0$) as for alkali-metal or alkaline-earth-metal atoms. The collision between two atoms is controlled by the electronic Born-Oppenheimer interaction potential(s) between them. All potentials are isotropic for the interaction of two S-state atoms. We restrict our discussion of molecular physics to such cases. Figure 7 shows as an example the $^1\Sigma_g^+$ and $^3\Sigma_u^+$ potentials for two ground state ^2S Li atoms, which are analogous to

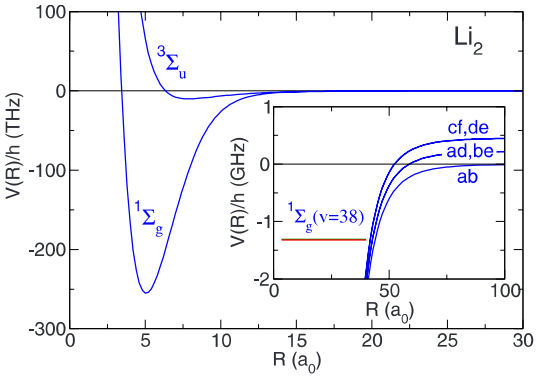

FIG. 7. (Color online) Molecular potentials $V(R)/h$ vs R of the two electronic states of Li_2 that correlate with two separated ^2S atoms. The inset shows an expanded view of the long-range s-wave potentials of ^{6}Li at $B=0$, indicating the five hyperfine states of the separated atoms (see Fig. 5) for which the total angular momentum has projection $M=0$. The inset also shows the last two nearly degenerate bound states (unresolved on the figure) of the $^6Li_2$ molecule from a coupled-channel calculation. It is a good approximation to label these nearly degenerate levels as the $I=0$ and 2 components of the total nuclear spin $\mathbf{I}=\mathbf{I}_1+\mathbf{I}_2$ of the last $v=38$ vibrational level of the $^1\Sigma_g^+$ potential.

the similar potentials for the H_2 molecule or other alkali-metal atoms. The superscripts 1 and 3 refer to singlet and triplet couplings of the spins of the unpaired electrons from each atom, i.e., the total electron spin $\mathbf{S}=\mathbf{S}_1+\mathbf{S}_2$ has quantum numbers $S=0$ and 1. The Σ refers to zero projection of electronic angular momentum on the interatomic axis for the S-state atoms, and g (u) refers to *gerade* (*ungerade*) electronic inversion symmetry with respect to the center of mass of the molecule. The g (u) symmetry is absent when the two atoms are not of the same species.

The Born-Oppenheimer potentials are often available from *ab initio* or semiempirical sources. When R is sufficiently small, typically less than $R_{ex}\approx 1$ nm for alkali-metal atoms, electron exchange and chemical bonding effects determine the shape of the potentials. For $R \gg R_{ex}$, the potentials are determined by the long-range dispersion interaction represented by a sum of second-order multipolar interaction terms.

1. van der Waals bound states and scattering

Many aspects of ultracold neutral atom interactions and of Feshbach resonances, in particular, can be understood qualitatively and even quantitatively from the scattering and bound state properties of the long-range van der Waals potential. The properties of this potential relevant for ultracold photoassociation spectroscopy have been reviewed by Jones *et al.* (2006). Its analytic properties are discussed by Mott and Massey (1965), Gribakin and Flambaum (1993), and Gao (1998b, 2000).

In the case of S-state atoms, the leading term in the long-range part of all Born-Oppenheimer potentials for a given atom pair has the same van der Waals potential characterized by a single C_6 coefficient for the pair. Consequently, all q_1q_2 spin combinations have the long-range potential

$$V_\ell(R) = -\frac{C_6}{R^6} + \frac{\hbar^2}{2\mu}\frac{\ell(\ell+1)}{R^2}. \tag{29}$$

A straightforward consideration of the units in Eq. (29) suggests that it is useful to define length and energy scales,

$$R_{vdW} = \frac{1}{2}\left(\frac{2\mu C_6}{\hbar^2}\right)^{1/4} \quad \text{and} \quad E_{vdW} = \frac{\hbar^2}{2\mu}\frac{1}{R_{vdW}^2}. \tag{30}$$

Gribakin and Flambaum (1993) defined an alternative van der Waals length scale which they called the mean scattering length,

$$\bar{a} = [4\pi/\Gamma(1/4)^2]R_{vdW} = 0.955\,978\ldots R_{vdW}, \tag{31}$$

where $\Gamma(x)$ is the gamma function. A corresponding energy scale is $\bar{E}=\hbar^2/(2\mu\bar{a}^2)=1.09\,422\ldots E_{vdW}$. The parameter $\bar{a}$ occurs frequently in formulas based on the van der Waals potential. Table I gives the values of R_{vdW} and E_{vdW} for several cases. Values of C_6 for other systems are tabulated by Tang *et al.* (1976), Derevianko *et al.* (1999), and Porsev and Derevianko (2006).

The van der Waals energy and length scales permit a simple physical interpretation (Julienne and Mies, 1989). A key property for ultracold collisions is that C_6/R^6 becomes large compared to the collision energy E when $R<R_{vdW}$. Thus, the wave function for any partial wave oscillates rapidly with R when $R<R_{vdW}$ since the local momentum $\hbar k(R)=\sqrt{2\mu[E-V(R)]}$ becomes large compared to the asymptotic $\hbar k$. On the other hand, when $R>R_{vdW}$, the wave function approaches its asymptotic form with oscillations on the scale determined by the long de Broglie wavelength of the ultracold collision. The energy scale E_{vdW} determines the nature of the connection between the long- and short-range forms of the wave function. The de Broglie wavelength $\lambda=2\pi(R_{vdW})$ for $E=E_{vdW}$. When $E\ll E_{vdW}$ so that $\lambda\gg R_{vdW}$, a WKB connection cannot be made near R_{vdW} between the asymptotic s wave and the short-range wave function [see Fig. 15 of Jones *et al.* (2006)]. Consequently, the quantum properties of the collision are manifest for $E<E_{vdW}$.

The van der Waals length also characterizes the extent of vibrational motion for near-threshold bound state. The outer turning point for classical motion for all low ℓ bound states is on the order of R_{vdW}. The wave function for $\ell=0$ oscillates rapidly for $R<R_{vdW}$ and decays exponentially as e^{-k_bR} for $R\gg R_{vdW}$, where $\hbar^2k_b^2/(2\mu)$ is the binding energy. The only case where the wave function extends far beyond R_{vdW} is that of the last s-wave bound state for the case of the universal halo molecule, where $a\gg R_{vdW}$ (see Secs. II.A and V.B.2).

The van der Waals potential determines the interaction over a wide zone between R_{vdW} and the much smaller R_{ex} where chemical forces become important. Thus, near-threshold bound and scattering state proper-